

# Interfacial Interaction between Dextran Sulfate and Lipid Monolayers: An Electrochemical Study<sup>†</sup>

Hélder A. Santos,<sup>‡</sup> Vladimir García-Morales,<sup>§</sup> Robbert-Jan Roozeman,<sup>‡</sup>  
José A. Manzanares,<sup>§</sup> and Kyösti Kontturi<sup>\*,‡</sup>

Department of Chemical Technology, Laboratory of Physical Chemistry and Electrochemistry,  
Helsinki University of Technology, P.O. Box 6100, FIN-02015 HUT, Finland, and  
Departament de Termodinàmica, Universitat de València, E-46100 Burjassot, Spain

Received December 21, 2004. In Final Form: April 1, 2005

The interaction between dextran sulfate (DS) with zwitterionic dipalmitoylphosphatidylcholine (DPPC) and negatively charged dipalmitoylphosphatidic acid monolayers at different surface pressures at air–liquid and liquid–liquid interfaces was studied using Langmuir–Blodgett (LB) and electrochemical techniques. The negatively charged DS can bind to phospholipids via calcium ions. To investigate the mechanism of the adsorption of DS on lipid monolayers, compression isotherms ( $\pi$ – $A$ ) and capacitance–potential curves were measured, and a theoretical model was developed to interpret the capacitance data. The compression of lipid monolayers in the presence of DS led to a more condensed hybrid layer, removing the LE–LC phase transition of DPPC. Lower surface pressures improved the binding of DS on the lipid monolayers via calcium bridges due to the electrostatic attraction. Alternating current voltammetry and cyclic voltammetry were used to monitor the transfer of a cationic  $\beta$ -blocker (metoprolol) across lipid monolayers in the absence and presence of the polyelectrolyte and to compare with the transfer of the standard probe, tetraethylammonium cation. Results showed a strong dependence on (i) the surface pressure, (ii) the applied potential, and, (iii) in the case of the hybrid layer, the charge of the phospholipid headgroup. Finally, results were also confirmed by attenuated total reflection Fourier transform infrared spectroscopy, performed after transferring lipid multilayers onto a solid substrate by the LB method.

## 1. Introduction

Over the past few years the study of the interactions between lipids and dextran sulfate (DS) has been of great interest.<sup>1–5</sup> As a result of the structural similarity between DS and glycosaminoglycans (GAGs), the interactions between lipids and GAGs can be studied using DS instead of GAGs. DS was found to carry out an important role as an anti-atherosclerotic drug,<sup>6</sup> as an anti-HIV infection agent,<sup>7</sup> and more recently in gene delivery systems.<sup>8–10</sup> However, some of those mechanisms of such actions are not well-understood yet.

GAGs which consist of highly sulfated and negatively charged polysaccharides are the major components in the extracellular matrixes (ECMs) of many tissues, but they can also be found inside and on the surface of cells.<sup>11</sup> GAGs

are structural and functional modulators of ECM and, therefore, extremely important to the development and repair of the central nervous system.<sup>12</sup> The incorporation of GAGs in well-defined structures, such as lipid monolayers, may provide interesting models for biological membranes, which can be used to study specific interactions. The knowledge of membrane structure, composition, and dynamics is very important to understand the biological phenomena and its functions.

DS is a polyelectrolyte (PE) exhibiting a well-known charge density along its flexible chain. Calcium ions can mediate the interaction between the negatively charged sulfate groups of DS molecules and zwitterionic or charged phospholipid headgroups<sup>3–5</sup> as a result of the attractive electrostatic forces between the charged PEs and the phospholipids<sup>1,13</sup> and repulsive forces between adsorbed DS strands.<sup>5</sup> Therefore, Ca<sup>2+</sup> mediated binding of GAGs to phospholipid layers has an important influence on lipid structure and lateral packing.<sup>4,5,14,15</sup> On the basis of NMR experiments, the smaller molecular area of lipid is ascribed to the headgroup tilt and to the increase of the lateral lipid packing density.<sup>4,5</sup> However, these studies have suggested no evidence of penetration of DS chains into the hydrophobic lipid membrane region.

Langmuir monolayers of lipids coupled to charged PEs have been used as well-defined model systems to study the interaction between PEs and phospholipid molecules at the air–liquid interface, as the molecular and charge density can easily be modified by compression or the choice

\* To whom correspondence should be addressed. Phone: +358 9 451 2570. Fax: +358 9 451 2580. E-mail: kontturi@cc.hut.fi.

<sup>†</sup> Abstract presented at the 55th annual meeting of the International Society of Electrochemistry, Greece-Thessaloniki, September 19–24, 2004.

<sup>‡</sup> Helsinki University of Technology.

<sup>§</sup> Universitat de València.

(1) Kim, Y. C.; Nishida, T. *J. Biol. Chem.* **1977**, *252*, 1243–1249.

(2) Kim, Y. C.; Nishida, T. *J. Biol. Chem.* **1979**, *254*, 9621–9626.

(3) de Meijere, K.; Brezesinski, G.; Zschörnig, O.; Arnold, K.; Möhwald, H. *Physica B* **1998**, *248*, 269–273.

(4) Huster, D.; Arnold, K. *Biophys. J.* **1998**, *75*, 909–916.

(5) Huster, D.; Paasche, G.; Dietrich, U.; Zschörnig, O.; Gutberlet, T.; Gawrlish, K.; Arnold, K. *Biophys. J.* **1999**, *77*, 879–887.

(6) Radhakrishnamurthy, B.; Ruitz, H. A.; Srinivasan, S. R.; Preau, W.; Dalferes, E. R.; Berenson, G. S. *Atherosclerosis* **1978**, *31*, 217–229.

(7) Bangham, A. D.; Hill, M. W.; Miller, N. G. A. *Science* **1988**, *240*, 646–649.

(8) Ruponen, M.; Ylä-Herttua, S.; Urtili, A. *Biochim. Biophys. Acta* **1999**, *1415*, 331–341.

(9) Wiethoff, C. M.; Smith, J. G.; Koe, G. S.; Middaugh, C. R. *J. Biol. Chem.* **2001**, *276*, 32806–32813.

(10) Ruponen, M.; Honkakoski, P.; Tammi, M.; Urtili, A. *J. Gene Med.* **2004**, *6*, 405–414.

(11) Schlessinger, J.; Lax, I.; Lemmon, M. *Cell* **1995**, *83*, 357–360.

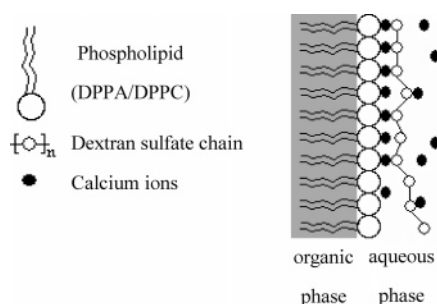
(12) Brittis, P. A.; Canning, D. R.; Silver, J. *Science* **1992**, *255*, 733–736.

(13) Srinivasan, S. R.; Lopez, A.; Radhakrishnamurthy, B.; Berenson, G. S. *Atherosclerosis* **1970**, *12*, 321–334.

(14) Huster, D.; Paasche, G.; Dietrich, U.; Gutberlet, T.; Zschörnig, O.; Gawrlish, K.; Arnold, K. *Chem. Phys. Lipids* **1990**, *55*, 301–307.

(15) Krumbiegel, M.; Arnold, K. *Chem. Phys. Lipids* **1990**, *54*, 1–7.

**Scheme 1. Schematic Drawing of the Interactions between the Lipid Surface and the Long DS Chain via Calcium Ion Bridges at the Aqueous–Organic Gel Interface**



of the subphase.<sup>16</sup> Electrochemical studies of monolayers at the interface between two immiscible electrolyte solutions have provided fundamental information of ion<sup>17–21</sup> and drug transfer<sup>17,22–25</sup> across the phospholipid monolayer, which can also be applied to the study of the hybrid lipid/DS system. By changing the charge density and distribution in the adsorption layer and in the monolayer, the effect of electrostatic interactions can be followed.

In this study, zwitterionic 1,2-dipalmitoylphosphatidylcholine (DPPC) and negatively charged 1,2-dipalmitoylphosphatidic acid (DPPA) were used as model membrane lipids, and negatively charged DS was used as the model for GAGs.<sup>3</sup> Calcium ions were used to create an attractive electrostatic interaction between lipid surfaces and DS. The interaction between DS and phospholipid monolayers, deposited on an immobilized aqueous–organic gel interface at different surface pressures, was followed measuring the compression isotherms and the capacitance of the monolayers. Also, the rate of transfer of tetraethylammonium (TEA<sup>+</sup>) and the cationic  $\beta$ -blocker, metoprolol, was measured as a function of the monolayer structure. To interpret the observed capacitance curves, a theoretical model was developed which describes the potential profile across a lipid monolayer in the absence and presence of DS. The model is an extension of our previous models, which allowed the main trends of the voltage–capacitance curves of some lipid monolayers<sup>25</sup> and PE multilayers deposited on liquid–liquid interfaces to be interpreted satisfactorily.<sup>17</sup> It is suggested that DS can couple to the lipid layer through calcium bridges as represented in Scheme 1.

Finally, to confirm the results, Fourier transform infrared (FTIR) spectroscopy was applied to verify the binding between the DS and the two phospholipids.

## 2. Theory

The interfacial region is modeled as a combination of three layers in series as shown in Figure 1. The organic

(16) de Meijere, K.; Brezesinski, G.; Möhwal, H. *Macromolecules* **1997**, *30*, 2337–2342.

(17) Slevin, C. J.; Malkia, A.; Liljeroth, P.; Toiminen, M.; Kontturi, K. *Langmuir* **2003**, *19*, 1287–1294.

(18) Kalkiuchi, T.; Kondon, T.; Kotani, M.; Senda, M. *Langmuir* **1992**, *8*, 169–175.

(19) Kontturi, A.-K.; Kontturi, K.; Murtoimäki, L.; Quinn, B.; Cunnane, V. J. *J. Electroanal. Chem.* **1997**, *424*, 69–74.

(20) Wandlowski, T.; Marecek, V.; Samec, Z. *J. Electroanal. Chem.* **1988**, *242*, 277–290.

(21) Koryta, J. *Electrochim. Acta* **1979**, *24*, 293–300.

(22) Mälkiä, A.; Liljeroth, P.; Kontturi, K. *Electrochim. Commun.* **2003**, *5*, 473–479.

(23) Mälkiä, A.; Liljeroth, P.; Kontturi, K. *Anal. Sci.* **2001**, *17*, i345–i348.

(24) Mälkiä, A.; Liljeroth, P.; Kontturi, A.-K.; Kontturi, K. *J. Phys. Chem B* **2001**, *105*, 10884–10892.

(25) Liljeroth, P.; Mälkiä, A.; Cunnane, V.; Kontturi, A.-K.; Kontturi, K. *Langmuir* **2000**, *16*, 6667–6673.

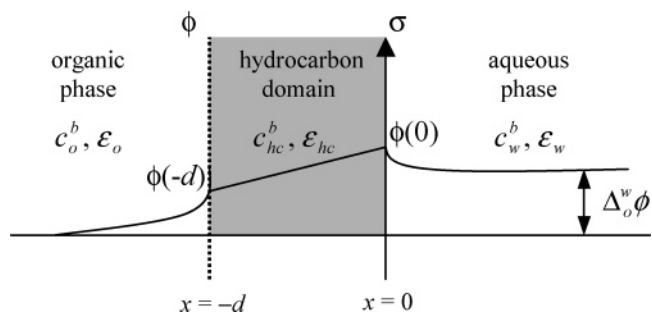


**Figure 1.** Schematic representation of the potential distribution across the interfacial region, including the coordinates and variables employed in the model.

and aqueous phases have bulk concentrations and relative permittivities of  $c_o^b$  and  $c_w^b$  and  $\epsilon_o$  and  $\epsilon_w$ , respectively. The hydrocarbon chains of the phospholipids occupy the region  $-d < x < 0$ , which is characterized by a relative permittivity  $\epsilon_{hc}$ . The ionic concentration in the hydrocarbon domain in the absence of potential difference,  $c_{hc}^b$ , is related to the bulk concentration in the organic phase through a partition coefficient  $K_p$ , so that  $c_{hc}^b = K_p c_o^b$ . For the sake of simplicity, the phospholipid headgroups, as well as the adsorbed dextran chains and calcium ions, are assumed to lie on the plane  $x = 0$ .

The electric potential distribution is described by the Poisson–Boltzmann equation<sup>25</sup>

$$\frac{d^2\varphi}{dx^2} = \kappa_o^2 \sinh \varphi, \quad x < -d \quad (1a)$$

$$\frac{d^2\varphi}{dx^2} = \kappa_{hc}^2 \sinh \varphi, \quad -d < x < 0 \quad (1b)$$

$$\frac{d^2\varphi}{dx^2} = \kappa_w^2 [e^{2(\Delta_o^w \varphi - \varphi)} - e^{-(\Delta_o^w \varphi - \varphi)}], \quad x > 0 \quad (1c)$$

where  $\varphi$  is the electric potential in  $RT/F$  units and measured with respect to the bulk organic phase,  $\Delta_o^w \varphi$  is the dimensionless electric potential in the bulk aqueous phase, and

$$\kappa_i \equiv \left( \frac{2F^2 c_i^b}{\epsilon_i RT} \right)^{1/2} \quad (2)$$

is the Debye parameter in region  $i$  ( $i = o, hc, w$ ). The boundary conditions for the electric displacement are

$$\epsilon_o \frac{d\varphi}{dx} \Big|_{x=-d^-} = \epsilon_{hc} \frac{d\varphi}{dx} \Big|_{x=-d^+} \quad (3a)$$

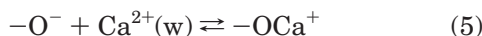
$$\epsilon_{hc} \frac{d\varphi}{dx} \Big|_{x=0^-} = \epsilon_w \frac{d\varphi}{dx} \Big|_{x=0^+} + \frac{F\sigma}{RT} \quad (3b)$$

where  $\sigma$  is the surface charge density at  $x = 0$  due to the phospholipid headgroups, the adsorbed calcium ions, and the adsorbed dextran chains. This is given by

$$\sigma = [z_{HG} + 2\alpha - \beta] \frac{e}{A} \quad (4)$$

where  $e$  is the elementary charge and  $A$  is the mean molecular area of phospholipids in the monolayer. The contribution from the headgroups,  $z_{HG}e/A$ , is 0 for the zwitterionic DPPC ( $z_{HG} = 0$ ) and  $-e/A$  for the negatively charged DPPA ( $z_{HG} = -1$ ); the measurements are carried

out at about pH = 7. At pH 7 DPPA molecules bear one negative charge due to the partial ionization of the phosphate group.<sup>26</sup> The contribution from the divalent calcium ions is  $2\alpha e/A$ , where  $\alpha$  is the degree of binding to any of the negatively charged oxygen radicals. The binding of a  $\text{Ca}^{2+}$  ion to an oxygen radical is assumed to follow the reaction



and the degree of binding  $\alpha$  can be obtained from the equilibrium equation

$$K_b = \frac{\alpha}{(1 - \alpha)c_w^b e^{2[\Delta_o^w \varphi - \varphi(0)]}} \quad (6)$$

where  $K_b$  is the binding constant. The value of this constant is taken from ref 27 as  $K_b = 400 \text{ M}^{-1}$ . Finally, the contribution from the adsorbed dextran chain is  $-\beta e/A$ , where  $\beta$  is considered to be a fitting parameter to be obtained from the comparison with the experimental capacitance versus potential curves (in particular, from the shift of the minimum in the capacitance curves). Obviously,  $\beta = 0$  in the absence of DS.

The solution of eqs 1a–4 yields the electric potential distribution through the interfacial region. Once this is known, the interfacial capacitance is calculated (by numerical differentiation) as

$$C = \frac{F}{RT} \frac{\partial Q}{\partial \Delta_o^w \varphi} \quad (7)$$

where

$$Q \equiv -\int_{-\infty}^0 \rho \, dx = \sigma + \int_0^{\infty} \rho \, dx \quad (8)$$

is the surface charge density separated across the liquid–liquid interface. This magnitude can be evaluated from the relation

$$\frac{F}{RT} Q = \int_{-\infty}^{-d} \epsilon_o \frac{d^2 \varphi}{dx^2} \, dx + \int_{-d}^0 \epsilon_{hc} \frac{d^2 \varphi}{dx^2} \, dx = 2(\kappa_o \epsilon_o - \kappa_{hc} \epsilon_{hc}) \sinh \frac{\varphi(-d)}{2} + 2\kappa_{hc} \epsilon_{hc} \sinh \frac{\varphi(0)}{2} \quad (9)$$

which is obtained after integration of eq 1a,b.

### 3. Experimental Section

**Materials.** The chemicals DPPC (Sigma, >99%), DPPA monosodium salt (Fluka, ≥98%), methanol (Merck, p.a.), 2-Nitrophenyl octyl ether (*o*-NPOE, Fluka, Selectophore), poly(vinyl chloride) (PVC, Sigma, very high molecular weight), chloroform (Merck, p.a.), tetraphenylarsonium chloride hydrate 97% (TPAsCl, Sigma, p.a.), tetrakis-4-chlorophenylborate (KTPBCl, Aldrich, p.a.), calcium chloride dihydrate ( $\text{CaCl}_2 \cdot 2\text{H}_2\text{O}$ , Merck, p.a.), tetraethylammonium chloride hydrate (Aldrich, p.a.), metoprolol tartrate (metoprolol, Sigma, reagent grade), and DS sodium salt from Leuconostoc ssp. (DS 500, Fluka, molecular weight 500 000) were all used as received without further purification. Figure 2 shows the chemical structure of PE DS.

Millipore Milli-Q water (resistivity > 18  $\text{M}\Omega \cdot \text{cm}$ ) was used to prepare all aqueous solutions and for rinsing.

**Methods.** *Langmuir–Blodgett Films.* DPPC and DPPA solutions were dissolved in chloroform and in chloroform/methanol

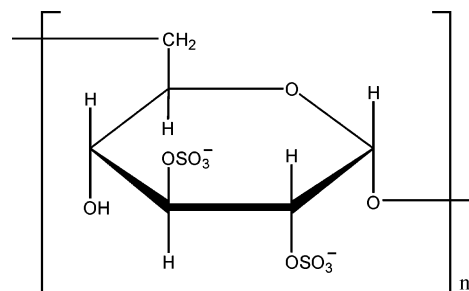
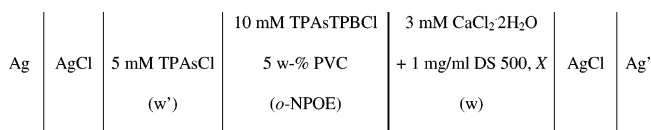


**Figure 2.** Molecular structure of DS represented in one of the three possible sulfate group forms.

(1:3), respectively, and used as spreading solutions. The typical solution concentration was 1 mg/mL. Surface pressure–molecular area ( $\pi$ – $A$ ) isotherms were measured with a computer interfaced Langmuir trough (length 300 mm, width 150 mm, KSV Instruments, Ltd., Helsinki) housed in an earthed Faraday cage. The subphase temperature was maintained constant at  $20.0 \pm 0.1$  °C. Lipid solutions were spread onto the aqueous  $\text{CaCl}_2$  subphase with the Hamilton syringe. The isotherms were recorded after the solvent had evaporated (30 min) with the compression speed of  $5.0 \text{ mm min}^{-1}$ . LB films were transferred by dipping the electrochemical cell perpendicularly through the lipid monolayer as described elsewhere.<sup>24,25</sup> The speed of the deposition was  $2.0 \text{ mm min}^{-1}$ . The success of the transfer was determined both from the electrochemical measurements and from the so-called transfer ratio, with values of about 75% and close to 100%, for lower and higher surface pressures, respectively. The surface pressures studied in this work were 32, 50, and 60 mN/m. As a result of the kinetic stability of the Langmuir monolayers, no changes in the monolayer properties were observed over several hours even after being deposited at a liquid–liquid interface.

**Electrochemical Measurements.** Alternating current (AC) impedance/voltammetry and cyclic voltammetry measurements were carried out using a four-electrode apparatus system<sup>28</sup> and an electrochemical cell. The details of the cell construction and setup can be found elsewhere.<sup>24,25</sup> Briefly, the cell was made of poly(tetrafluoroethylene) with an interfacial area of  $0.28 \text{ cm}^2$ . For the preparation of the organic gel phase a mixture of 5 wt % PVC and *o*-NPOE containing the base electrolyte was heated at least to 110 °C, and the resulting hot gel was simply cast into the cell. Typically, the solidification of the gel was carried out overnight. Calcium chloride dihydrate was used as an aqueous base electrolyte, and TPAsCl was used as the organic reference electrolyte. As described in detail elsewhere,<sup>29</sup> the organic base electrolyte TPAsTPBCl was obtained by precipitation from equimolar solutions of TPAsCl and KTPBCl. Ag/AgCl reference electrodes were used for the electrochemical measurements, and the auxiliary electrodes were Pt wires.

The electrochemical cell used can be represented as follows:



where X is either  $\text{TEA}^+$  or metoprolol in a concentration of about 50  $\mu\text{M}$ .

The cell interface was positioned between two Luggin capillaries to minimize the ohmic drop. All electrochemical experiments were carried out inside of a grounded Faraday cage with the Autolab PGSTAT100 (EcoChemie B. V., The Netherlands) at  $20.0 \pm 0.1$  °C. Cyclic voltammetry measurements were carried out at sweep rates of 25, 50, 75, and 100 mV/s. AC voltammetry was measured at the frequencies of 5, 10, 20, 25, and 30 Hz, using the sweep rate of  $1 \text{ mV s}^{-1}$ , and the amplitude of 5 mV (root

(26) Jacobson, K.; Papahadjopoulos, D. *Biochemistry* **1975**, *14*, 152–161.

(27) Tatulian, S. A. In *Surface Chemistry and Electrochemistry of Membranes*; Sørensen, T. S., Ed.; Marcel Dekker: New York, 1999; p 898.

(28) Vanýsek, P. *Modern Technique in Electrochemistry*; John Wiley & Sons: New York, 1996; Vol. 139, Chapter 8.

(29) Cunnane, V. J.; Schiffrin, D. J.; Beltran, C.; Geblewicz, G.; Solomon, T. J. *Electroanal. Chem.* **1988**, *247*, 203–214.

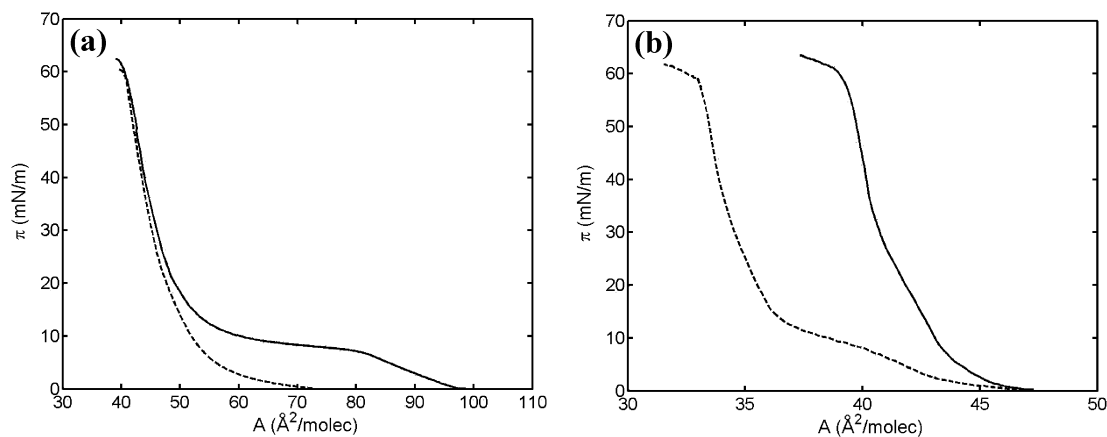


**Figure 3.** Surface pressure versus molecular area isotherms of DPPC (a) and DPPA (b) at air–water interface on the 3 mM  $\text{Ca}^{2+}$  aqueous subphase in the absence (solid line) and in the presence of coupled lipid/ $\text{Ca}^{2+}$ /DS complexes (dotted line) at  $T = 20 \pm 0.1$  °C.

mean square), with a modulation and interval time of 0.4 s and 1 s, respectively. All measurements were carried out using aqueous 3 mM  $\text{CaCl}_2$  solutions, which is the approximate extracellular concentration of  $\text{Ca}^{2+}$  ions,<sup>5</sup> and a DS concentration of 1 mg/mL as described elsewhere.<sup>3,30</sup>

**Attenuated Total Reflection (ATR)-FTIR Measurements.** To confirm the adsorption of DS, ATR-FTIR measurements were performed. For that purpose the LB technique was used to transfer the films onto a solid substrate. The FTIR measurements were carried out on a Bruker IFS113v spectrometer equipped with a liquid nitrogen cooled mercury cadmium telluride detector and a Specac 6 reflection ATR accessory. Typically four layers of lipid (DPPC) were deposited on the Ge ATR element at the surface pressures of 50 and 60 mN/m, in the absence and presence of DS. Control measurements were also performed on the DPPA system. The signal-to-noise ratio of the spectra was improved by averaging 256 interferograms with a resolution of  $4\text{ cm}^{-1}$ . A three-term Blackman-Harris apodization function and a zero-filling factor of 2 were used in processing the interferogram. Measurements were carried out under a vacuum to minimize the contribution of the water bands. A spectrum of the clean ATR element was used as a background reference.

#### 4. Results and Discussion

**Isotherms.** Figure 3 shows the compression isotherms of DPPC (a) and DPPA (b) in the absence and in the presence of DS. From the recorded  $\pi$ - $A$  isotherms of the phospholipids at the air–liquid interface in the absence and presence of DS, the surface compressibility modulus ( $C_s^{-1}$ ) of the monolayer can be calculated according to the equation<sup>31</sup>

$$C_s^{-1} = -A \left( \frac{\partial \pi}{\partial A} \right)_T \quad (10)$$

The isotherm for the pure DPPC monolayer showed characteristic phases consistent with the literature:<sup>32–35</sup> a gaseous phase at  $A > 100\text{ \AA}^2$  and a liquid-expanded (LE) phase at  $A = 77\text{--}100\text{ \AA}^2$ . At the surface pressure of about 5 mN/m a plateau corresponding to the first-order phase transition between the LE and a liquid-condensed (LC)

phase is observed, but the formation of the DPPC/ $\text{Ca}^{2+}$ /DS complex removes this transition. This suggests that due to the formation of the complex<sup>4,5</sup> in the air–water interface (see Figure 3a) DS molecules do not penetrate into the lipid monolayer, because there is no increase of the surface pressure<sup>11</sup> at large molecular areas.<sup>36</sup> This indicates the binding between lipid and DS by Coulomb interactions mediated by  $\text{Ca}^{2+}$  ions as was demonstrated elsewhere<sup>4,5</sup> and, thus, the adsorption of DS at the surface only. Yet, at the collapse point, both the molecular area and the collapse pressure are slightly decreased with the formation of the DPPC/ $\text{Ca}^{2+}$ /DS complex, from 52 to 50  $\text{\AA}^2$  and from 64 to 61 mN/m, respectively.

The binding of the PE leads to a less expanded isotherm, which can be owed to the increase of the lateral lipid density.<sup>3</sup> Thus, the difference in the surface compressibility ( $337 \pm 2\text{ mN/m} > 273 \pm 2\text{ mN/m}$ , calculated at the LC phase) can be explained by the closest packing of the lipid molecules in the absence of DS resulting from strong cohesive interactions between the carbon chains. On the other hand, at higher pressures ( $\approx 60\text{ mN/m}$ ), the compression isotherms of DPPC exhibit the same molecular area in the absence and presence of DS, which can be explained by the break in the electrostatic calcium bridge between the negatively charged DS strands and the lipid monolayer,<sup>30</sup> leading to desorption of DS from the surface; this is discussed later on.

In contrast, the negatively charged lipid (DPPA, see Figure 3b) isotherm is typical for many lipids with sufficiently strong van der Waals attraction to prevent a LE phase<sup>11</sup> and, thus, does not display a fluid phase. At the very low surface pressure (3 mN/m) a change in the slope at  $A = 43\text{ \AA}^2$  was observed for the DPPA/ $\text{Ca}^{2+}$ /DS hybrid layer, which indicates the formation of a LE phase, and, thus, an inflection point is observed corresponding to the phase transition from the gaseous–LE coexistence phase to the LC phase, which is in good agreement with the literature.<sup>16,37</sup> Furthermore, the PE coupled to charged lipid monolayers shifts the isotherm to much smaller molecular areas and, thus, the isotherm of the lipid/ $\text{Ca}^{2+}$ /DS complex was about 6.3  $\text{\AA}^2/\text{molecule}$  more condensed compared to the pure lipid isotherm, which indicates strong adsorption between negatively charged DS and DPPA at the air–liquid interface. The molecular area at the phase transition is about 36  $\text{\AA}^2$  in the presence of DS,

(30) Zschörnig, O.; Richter, W.; Paasche, G.; Arnold, K. *Colloid Polym. Sci.* **2000**, *278*, 637–646.

(31) Petty, M. C. *Langmuir-Blodgett: An introduction*; Cambridge University Press: New York, 1996.

(32) Ravaine, S.; Fanucci, G. E.; Seip, C. T.; Adair, J. H.; Talham, D. R. *Langmuir* **1998**, *14*, 708–713.

(33) Koynova, R.; Caffrey, M. *Biochim. Biophys. Acta* **1998**, *1376*, 91–145.

(34) Mitchell, M. L.; Dluhy, R. A. *J. Am. Chem. Soc.* **1988**, *110*, 712–718.

(35) Zhang, J.; Unwin, P. R. *J. Am. Chem. Soc.* **2002**, *124*, 2379–2383.

(36) Brun, A.; Brezesinski, G.; Möhwald, H.; Blanzat, M.; Perez, E.; Rico-Lattes, I. *Colloids Surf., A* **2003**, *228*, 3–16.

(37) Meijere, K.; Brezesinski, G.; Möhwald, H. *Langmuir* **1998**, *14*, 4204–4209.

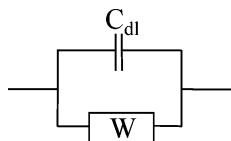


**Figure 4.** Equivalent electrical circuit used in this study to calculate the interfacial capacitance:  $C_{dl}$  is the double layer capacitance, and  $W$  is the Warburg impedance.

and more pronounced features are observable in the isotherm, while in the absence of DS it is about  $42 \text{ \AA}^2$ .

Close to the point of collapse, the molecular area of the hybrid layer is slightly lower (ca.  $62 \text{ mN/m}$ ) than that of the pure lipid isotherm (ca.  $64 \text{ mN/m}$ ). The surface compressibilities of DPPA + DS and DPPA monolayers have higher values ( $823 \pm 5$  and  $962 \pm 5 \text{ mN/m}$ , respectively, calculated at the LC phase) than the DPPC monolayers, which can be explained by the presence of  $\text{Ca}^{2+}$  ions increasing the electrostatic interactions and leading to a more packed system, consequently resulting in the strong adsorption of DS and the formation of higher ordered lipid structure. The close packing of the DPPA + DS hybrid layer is less than that of the DPPA monolayer, resulting from weak cohesive interactions between the carbon chains and due to the repulsive interactions between the negatively charged coupled complexes at very high surface pressures.

**Capacitance Studies.** The interaction of the lipid monolayer with DS present in the bulk solution was also studied electrochemically. For that purpose, AC voltammetry was applied to measure the interfacial capacitance as the function of the applied potential in the presence of the base electrolytes only. Considering that the transfer of the base electrolyte ions is diffusion-limited, the equivalent electric circuit in Figure 4 was used, that is, assuming that the solution resistance had completely been compensated for by the positive feedback.<sup>24</sup> Thus, the interface was modeled as the parallel combination of a capacitor and a Warburg impedance. Hence, the admittance of the interface,  $Y$ , is

$$Y = \frac{\sqrt{j\omega}}{\sigma} + j\omega C \quad (11)$$

where  $\omega$  is the angular frequency of the applied ac potential,  $\sigma$  is the coefficient of the Warburg impedance, and  $C$  is the interfacial capacitance. Thus, the interfacial capacitance can be calculated by rearranging eq 11 into real and imaginary components:<sup>38</sup>

$$\omega C = Y'' - Y' \quad (12)$$

where  $Y''$  and  $Y'$  are the imaginary and the real components of a measured total admittance, respectively.

Figure 5 shows the measured capacitance versus potential curves of DPPC and DPPA monolayers at different surface pressures in the absence and presence of DS.

In Figure 5a,c, curves for DPPC and DPPC + DS are shown. Calcium ion binding to the zwitterionic headgroup of DPPC creates a positive charge density at the interface ( $x = 0$ ) and, therefore, shifts the minimum of capacitance curves to more negative values. Addition of DS to the aqueous solution and its subsequent adsorption to the interface influence the capacitance curves in three ways: (i) shift of the minimum to more positive potentials, (ii) increased capacitance at low potentials, and (iii) lower

**Table 1.** Values of the Fitting Parameters in the Calculated Capacitance Curves

	$\pi$ (mN/m)	$\epsilon_{hc}$	$K_p$	$\beta$
DPPC	32	12	0.03	
	50	10	0.03	
	60	8	0.03	
DPPC + DS	32	6	0.5	0.4
	50	5	0.5	0.2
	60	3	0.5	0.1
DPPA	32	16	0.02	
	50	8	0.02	
	60	3	0.004	
DPPA + DS	32	7	0.1	0.3
	50	6	0.1	0.4
	60	3	0.006	0.0

value of the minimum capacitance. These three trends occur in both DPPC and DPPA and can be understood from the theoretical model. In Figure 5b,d, curves for DPPA and DPPA + DS are shown. The minimum of the capacitance curves is now shifted to more positive potentials, as should be expected because the headgroup of this lipid is negatively charged. Again, binding of calcium ions occurs but the net surface charge density is lower.

The theoretical model includes three fitting parameters,  $\epsilon_{hc}/d$ ,  $K_p$ , and  $\beta$ , whose physical meaning can be clearly understood. The ratio  $\epsilon_{hc}/d$  is the geometric capacitance of the hydrocarbon domain. In our calculations, we have kept constant the thickness of the hydrocarbon domain as  $d = 6 \text{ \AA}$ . Values used for other parameters are  $\epsilon_o = 24.2$  (ref 25) and  $\epsilon_w = 78.54$  (ref 39). An increase in the surface pressure of the phospholipid monolayer lowers the effective dielectric constant of this domain and decreases the capacitance minimum.<sup>17</sup> A low value of the partition coefficient  $K_p$  implies a strong exclusion from the hydrocarbon region of the mobile ions coming from the organic phase, and it is also related to attaining a more compact structure. Increasing the partition coefficient  $K_p$  leads to a higher capacitance as the potential moves away from the capacitance minimum, because charge coming from the organic phase is then allowed to flow to the interface increasing the capacitance far from the minimum. Finally, the parameter  $\beta$  describes the dextran adsorption and allows us to reproduce the shift of the capacitance minimum to more positive potentials.

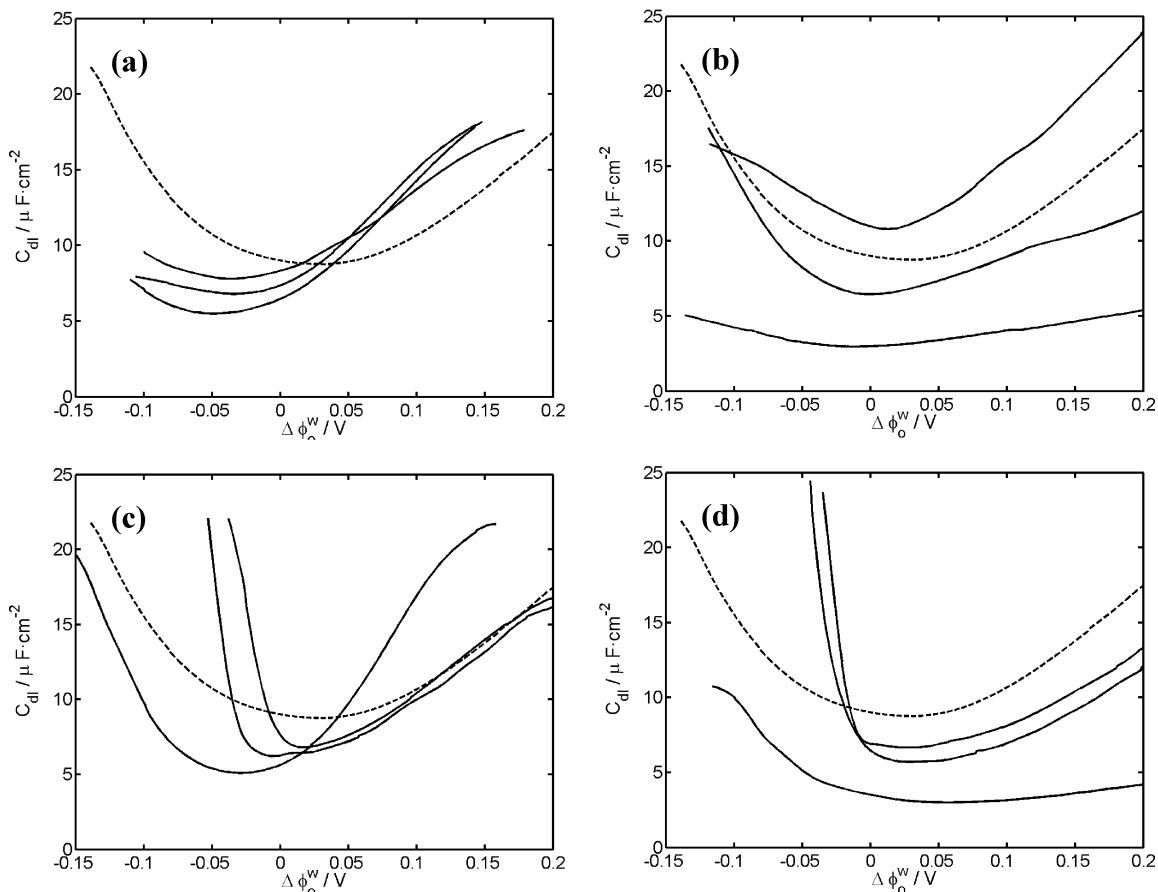
In Table 1, values for all fitting parameters are tabulated. These values arising from the theoretical model allow qualitatively the trends observed to be explained, thus, providing insight into the interactions.

Figure 6a shows the capacitance curves for a DPPC monolayer in the absence of DS calculated from the solution of eqs 1–7. Because the headgroups are zwitterionic at the  $\text{pH} \approx 7$  of the measurements, the fact that the minimum of the capacitance curves lies at negative potentials is interpreted as an evidence of calcium binding. When the surface pressure is increased, the capacitance minimum decreases due to a decrease of the effective dielectric constant of the hydrocarbon domain.

Figure 6c shows the calculated capacitance curves of DPPC monolayers in the presence of DS. The addition of DS shifts the minimum of the capacitance curves to more positive values, which evidences the adsorption of negatively charged dextran chains. When the surface pressure is increased, the value of the fitting parameter  $\beta$  (which describes dextran adsorption) decreases. That is, when the pressure increases, the lipid layer becomes more compact and releases part of the adsorbed DS chains.

(38) Kakiuchi, T.; Senda, M. *Collect Czech. Chem. Commun.* **1991**, *56*, 112–129.

(39) Osaki, T.; Ebina, K. In *Liquid Interfaces in Chemical, Biological and Pharmaceutical Applications*; Volkov, A. G., Ed.; Marcel Dekker: New York, 2001; p 23.



**Figure 5.** Measured capacitance curves of DPPC (a, c) and DPPA (b, d) monolayers at the aqueous–organic gel interface at the surface pressures of 32, 50, and 60 mN/m (continuous lines from top to bottom), in the absence (a, b) and in the presence of DS (c, d). The dashed line corresponds to a bare interface.

The effective dielectric constant of the hydrocarbon domain decreases after DS addition. This is equivalent to an increase of the thickness of this region (since the geometric capacitance  $\epsilon_{\text{h}}d$  is the physically relevant parameter) and is consistent with ellipsometric measurements in zwitterionic DPPE monolayers which showed an increase of the film thickness after dextran addition.<sup>3</sup>

In Figure 5c it can be observed that DS addition increases the curvature of the experimental capacitance curves. In our theoretical model, this curvature is controlled by the partition coefficient so that the higher the curvature the higher the partition coefficient. It is known that the tilt angles of the DPPA hydrocarbon tails increase after addition of PE poly(diallyldimethylammonium chloride),<sup>16</sup> and this creates some available space between the chains for the incorporation of organic ions. A similar structural change could be responsible for our observations after DS addition.

The calculated capacitance curves of DPPA monolayers in the absence and presence of DS are presented in parts b and d of Figure 6, respectively. They follow trends similar to those observed in DPPC monolayers, with the only exception of the nonmonotonic trend of  $\beta$ . It seems that in DPPA electrostatic interactions through  $\text{Ca}^{2+}$  bridges dominate over entropic effects at pressures lower than 60 mN/m. This means that increasing pressure leads to a higher concentration of these bridges and, hence, to a better absorption of DS (thus increasing  $\beta$ ). At a pressure equal to 60 mN/m desorption of DS chains takes place and the value of  $\beta$  decreases. On the contrary, entropic effects can be more important in DPPC than electrostatic interactions at increasing pressures leading to the release

of DS chains, and this leads to a monotonic decrease of  $\beta$  with increasing pressure.

A slight asymmetry is observed in the experimental curves compared to the theoretical ones. We found in previous calculations that this asymmetry can be reproduced considering that the dextran layer has a finite thickness and that another plane of charge is located in the aqueous phase (arising from the unbound dextran chains). Because the conclusions remain unchanged we have decided to focus on the main features and not to introduce additional free parameters to describe the asymmetry. These make reference to the position of the minimum and its shift after adding dextran, as well as the origin of the more noticeable changes in the curvature of the capacitance curves.

Cyclic voltammetry was also employed to confirm the qualitative interpretation of the previous discussion. The cyclic voltammograms of a DPPA monolayer deposited at different surface pressures coupled to DS in the aqueous solution at a sweep rate of 75 mV/s are shown in Figure 7. At about  $\Delta\phi_o^w = -0.1$  V, close to the negative limit of the polarization window, where  $\text{TPBCl}^-$  is transferred from oil to water phase, an additional current wave is observed after the addition of DS. This current is attributed to the adsorption of dextran onto the lipid monolayer for surface pressures < 60 mN/m, as the peak separation is almost 0. At the surface pressure of 60 mN/m voltammograms are similar to those measured in the absence of DS, which indicates that DS chains are partially desorbed from the interface. Thus, these results are in good agreement with the AC voltammetry measurements and the previous discussion.

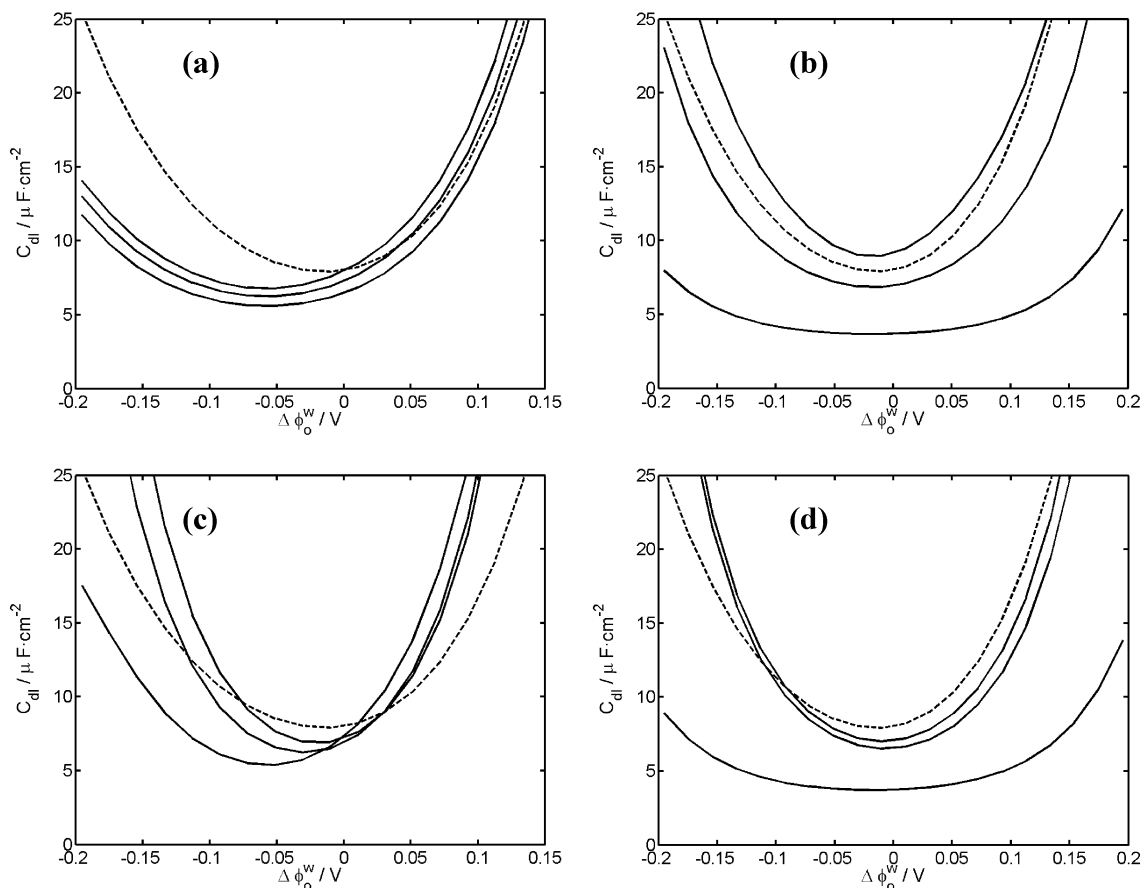


**Figure 6.** Calculated capacitance curves of DPPC (a, c) and DPPA (b, d) monolayers at the aqueous–organic gel interface at the surface pressures of 32, 50, and 60 mN/m (continuous lines from top to bottom), in the absence (a, b) and in the presence of DS (c, d). The dashed line corresponds to a bare interface. Values of the fitting parameters have been taken from Table 1.

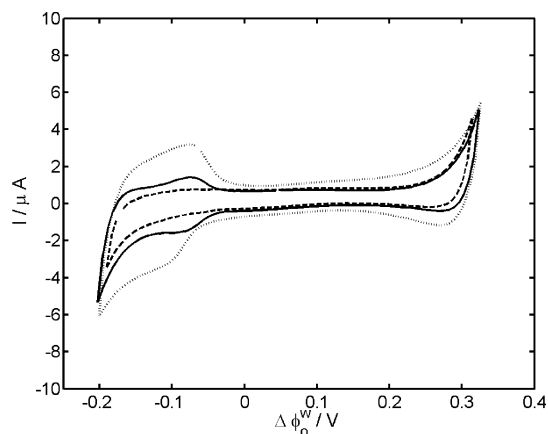


**Figure 7.** Cyclic voltammograms at a sweep rate of 75 mV/s of a DPPA monolayer in the presence of DS via calcium bridges deposited at  $\pi = 32$  mN/m (solid line), 50 mN/m (dotted line), and 60 mN/m (dashed line).

**Ion Transfer Studies.** To assess the applicability of the present system in mimicking the cell membrane, ion transfer across the monolayers was studied with AC and cyclic voltammetry, using TEA<sup>+</sup> and metoprolol as the probe cations. Figure 8a,b plots the capacitance curves calculated from eq 12 as a function of the applied potential for the ion transfer of TEA<sup>+</sup> and metoprolol across DPPC (Figure 8a) and DPPA (Figure 8b), respectively; monolayers were deposited at  $\pi = 50$  mN/m in the absence and presence of DS.

Mälkiä et al.<sup>24</sup> have studied the drug and ion transfer across distearoyl phosphatidylcholine monolayers, and

more recently Slevin et al.<sup>17</sup> have also done similar work using PE multilayers and a cationic lipid monolayer of dioleoyltrimethylammoniumpropane. The first authors have demonstrated that some drug molecules such as tacrine, propranolol, or metoprolol and ions such as TEA<sup>+</sup> interact with the lipid monolayer in such a way that TEA<sup>+</sup> shows a similar affinity for both sides of the model membrane while metoprolol is more attracted to the hydrocarbon chain. Metoprolol and tacrine are also more strongly membrane active than propranolol.

The presence of DS has a strong effect on the ion transfer across the lipid monolayers. As can be seen, the addition of DS lowers the capacitance, due to the increase of the real component of the admittance (results not shown), which indicates enhanced adsorption and the presence of kinetic limitations.<sup>24</sup> The lipid/Ca<sup>2+</sup>/DS complex shifts the potential of zero charge (or the potential of the minimum capacitance) toward more positive potentials, probably due to the reorientation and electrostatic interactions between the phospholipid molecules and the ions at the interface. Also, the adsorption of DPPC (see Figure 8a) is slightly weaker than that of the charged lipid DPPA (Figure 8b).

Figure 9 shows the cyclic voltammograms of TEA<sup>+</sup> (a, b) and metoprolol (c, d) ion transfer across DPPA monolayers deposited at the surface pressure of 50 mN/m in the absence (a, c) and presence (b, d) of DS. After subtraction for the current due to the base electrolytes only, the peak currents for both cations were proportional to the square root of the scan rate fairly well (results not shown). Hence, it can be concluded that the ion transfer is under mixed kinetic and diffusion control. On the other

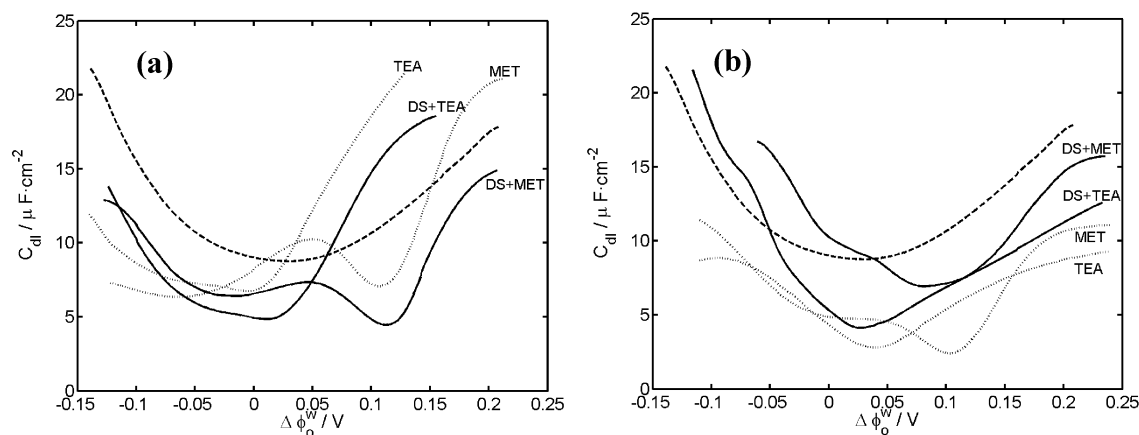


**Figure 8.** Plots of the capacitance curves as a function of the applied potential at the aqueous–organic gel interface for the ion transfer across DPPC (a) and DPPA (b) monolayers deposited at  $\pi = 50$  mN/m. The dashed line corresponds to a bare interface. Labels indicate the ion which is transferred in each case and the absence (dotted lines) or presence (solid lines) of DS.

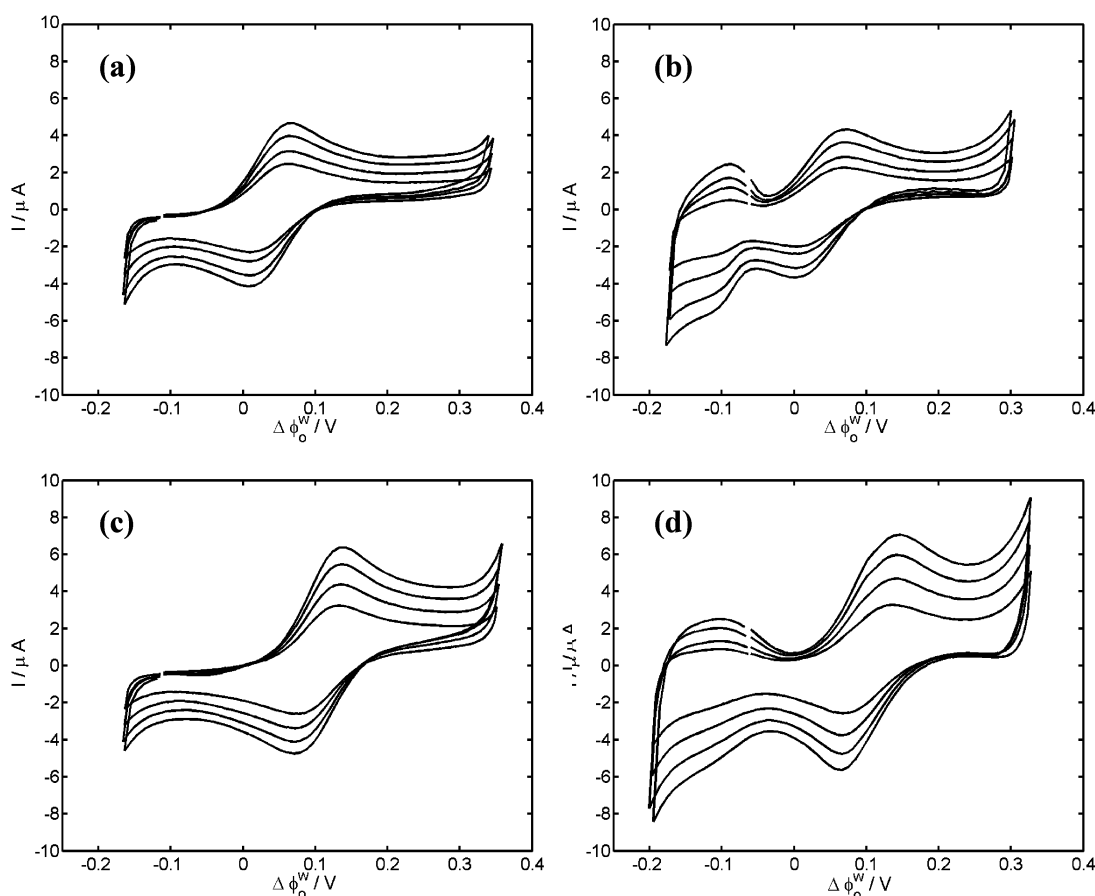


**Figure 9.** Cyclic voltammograms of TEA<sup>+</sup> (a, b) and metoprolol (c, d) transfer across DPPA monolayers deposited at 50 mN/m in the absence (a, c) and presence (b, d) of DS. Scan rates of 25, 50, 75, and 100 mV/s (from the bottom to the top).

hand, the increase in the current at more negative potentials in the presence of DS is explained by the adsorption of negatively charged dextran chains to the lipid monolayer, as the peak separation is practically zero (see also Figure 7).

The apparent contradiction that in the calculation of the capacitance a simple circuit in Figure 4 was used while in the cyclic voltammograms partial kinetic control is observed requires a couple of comments: in AC voltammetry, no transferring ion was present, and it is easy to show that as the measurements are carried out at several hundreds of millivolts away from the standard transfer

potentials of the base electrolytes, the Warburg element overcomes the charge transfer resistance by a factor of hundreds. Thus, the simple circuit is a good approximation. In ion transfer studies, a third branch in parallel with those in Figure 4, consisting of a series combination of the charge transfer resistance and the Warburg element of the transferring ion, must be considered. Having subtracted for the base electrolyte current, also the capacitive current component has been removed and the current due to the trace ion only is revealed, showing both the kinetic and diffusion resistance.<sup>38</sup>

**Table 2. Apparent Rate Constants for TEA<sup>+</sup> and Metoprolol Transfer Across the Lipid Monolayer Deposited at a Surface Pressure of 50 mN/m in the Absence and Presence of DS**

lipid monolayer	ion transfer ( $k_{app}^0$ , cm <sup>2</sup> ·s <sup>-1</sup> )	
	TEA <sup>+</sup>	metoprolol
DPPC	0.092	0.0066
DPPC+DS	0.013	0.018
DPPA	0.052	0.0046
DPPA+DS	0.033	0.021

Thus, kinetic parameters can be determined using the method of Nicholson and Shain applying the equation<sup>40</sup>

$$\psi = \frac{(D_w/D_o)^{\alpha/2} k_{app}^0}{[\pi D_w f \nu]^{1/2}} \quad (13)$$

where  $f = nF/RT$ ,  $D_w$  and  $D_o$  are the water and the oil diffusion coefficients of the transferring ion, respectively,  $\alpha$  is the transfer coefficient for which the value of 0.5 is assumed, and  $\nu$  is the scan rate. Using the values from ref 40, the kinetic parameter,  $\psi$ , can be related to the peak separation and, hence, to the effective rate constant,  $k_{app}^0$ . Before each ion transfer measurement, voltammograms were corrected for the base electrolyte current. The transfer coefficients  $D_w$  and  $D_o$  of TEA<sup>+</sup> and metoprolol obtained for a PVC gel phase were reported to be  $1.0 \times 10^{-5}$  and  $4.8 \times 10^{-7}$  cm<sup>2</sup>·s<sup>-1</sup> and  $5.9 \times 10^{-6}$  and  $1.3 \times 10^{-7}$  cm<sup>2</sup>·s<sup>-1</sup>, respectively, for the aqueous–organic gel interface.<sup>24</sup> As a result of the similarity of the systems the same values were used. Table 2 shows the apparent rate constants for TEA<sup>+</sup> and metoprolol transfer across the lipid monolayer deposited at a surface pressure of 50 mN/m in the absence and presence of DS calculated from the CVs (see Figure 9) and applying eq 13. The results are consistent with the fact that lower rate constants are expected for larger molecules.<sup>41</sup> Thus, the rate constant value of metoprolol is rather low when compared with that of TEA<sup>+</sup>, taking into account the molecular radius of those molecules in nanometers, 0.434 (ref 24) and 0.337 (ref 42), respectively. The apparent rate constants are strongly dependent on the phospholipid headgroup charge and the presence of DS molecules coupled to the lipid monolayer. The rate constant for DPPC/Ca<sup>2+</sup>/DS complexes has a lower value than for the pure lipid monolayer only, which is understood by the increased difficulty of the ion transfer across a more densely packed interface due to the adsorption of the PE on the lipid surfaces (via calcium bridges). However, for the metoprolol transfer across lipid/Ca<sup>2+</sup>/DS complexes, the apparent rate constant was higher than in the absence of the coupled system. The explanation for such a result is not clear yet, but our results suggest a more complex interaction between the cationic  $\beta$ -blocker and the lipid monolayer coupled to DS, as was previously reported.<sup>24,43</sup> Furthermore, the formation of lipid/Ca<sup>2+</sup>/DS complexes may facilitate the metoprolol transfer across the lipid monolayer to some extent, while for pure lipid monolayers the excess of free negative charge at the surface might lead to electrostatic binding with the metoprolol positively charged, thus, leading to a slight decrease in the rate constant.

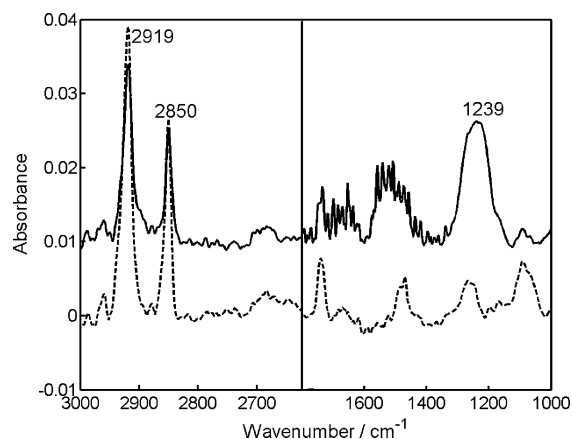


**Figure 10.** ATR-FTIR spectra of DPPC multilayers deposited at a surface pressure of 50 mN/m in the absence (dotted line) and in the presence (solid line) of DS. Offset for clarity.

**ATR-FTIR Measurements.** To verify the interactions between the DS and the two phospholipids, ATR-FTIR experiments were carried out on deposited multilayers of DPPC (Figure 10) and DPPA. Here we shall report mainly on the data of DPPC, because of the well-known characterization of DPPC in the literature by IR spectroscopy, and, thus, a better comparison with our data can be made. In our experiments, two different deposition surface pressures were used (50 and 60 mN/m) and four layers of lipid were successfully transferred onto a solid substrate.

Figure 10 shows the ATR spectra of DPPC in the absence and presence of DS. In the spectra the absorption bands for the symmetric and asymmetric stretching of the methylene group,  $\nu_s = 2850$  cm<sup>-1</sup> and  $\nu_a = 2919$  cm<sup>-1</sup>, are easily distinguished. Moreover, the band centered at 1269 cm<sup>-1</sup> has been assigned to asymmetric P=O stretching of the PO<sub>2</sub><sup>-</sup> group.<sup>44</sup> After inclusion of dextran in the subphase, a broad band around 1239 cm<sup>-1</sup> appears which almost covers the P=O stretching band. This has been assigned to the asymmetric stretching of the S=O.<sup>45</sup> It shows that dextran must be an integral part of the transferred monolayers system, as was suggested already by the AC voltammetry measurements. Another observation is that whereas the lipid-only spectrum shows negligible water bands, the lipid–dextran spectrum contains medium water bands around 1640 cm<sup>-1</sup>. This means that water molecules are included in the dextran–phospholipid multilayer. At the same time this water content explains the decrease in spectral intensity of the characteristic lipid bands. This supports our previous discussion that for lower surface pressures DS is adsorbed to the transferred monolayers. From the DPPA measurements a similar behavior was observed (results not shown).

## 5. Conclusions

These preliminary results have showed that the interactions between lipid/Ca<sup>2+</sup>/DS complexes can be electrochemically monitored and such interactions are strongly dependent on the surface pressure, the applied potential, and, in the case of the hybrid layer, the lipid headgroup. We have studied the capacitance curves through a theoretical model that allows us to explain the main trends observed. It has been shown that calcium ion binding to the headgroups, partial ion exclusion from the hydrocarbon domain, and complexation of the negatively charged

(40) Nicholson, R. S. *Anal. Chem.* **1965**, *37*, 1351–1355.

(41) Ferrigno, R.; Girault, H. H. *J. Electroanal. Chem.* **2001**, *496*, 131–136.

(42) Marcus, Y. *Ion Solvation*; Wiley: Chichester, 1985.

(43) Herbette, L.; Katz, A. M.; Sturtevant, J. M. *Mol. Pharmacol.* **1983**, *24*, 259–269.

(44) Cevc, G. *Phospholipids Handbook*; Marcel Dekker: New York, 1993.

(45) Cabassi, F.; Casu, B.; Perlin, A. S. *Carbohydr. Res.* **1978**, *63*, 1–11.

dextran chains with the lipid headgroups through calcium bridges are the essential phenomena that explain the observed behavior. The addition of DS has mainly two effects: (1) makes the surface charge concentration more negative (shift of the minimum to the right) and (2) enhances the concentration of small ions coming from the organic phase to the region where the hydrocarbon (hydrophobic) tails are located, which is modeled as a different medium with a low dielectric constant (this leads to a higher capacitance).

Future goals include the incorporation and characterization of pore-forming peptides in the model membrane system. In addition, the approach of employing comple-

mentary techniques, such as fluorescence anisotropy, will be revived to obtain more detailed information on the structure and dynamics of the lipid monolayer at the liquid–liquid interface.

**Acknowledgment.** Financial support from European Union under the research and training network SUSANA (“Supramolecular Self-Assembly of Interfacial Nanostructures”, Contract Number HPRN-CT-2002-00185) is gratefully acknowledged. Dr. Lasse Murto $\ddot{m}$ äki is also acknowledged for helpful discussions.

LA046825U